Carbohydrate Polymers 86 (2011) 1558–1564

Contents lists available at ScienceDirect

Carbohydrate Polymers

journal homepage: www.elsevier.com/locate/carbpol

Biosynthesis of spherical Fe_3O_4/bacterial cellulose nanocomposites as adsorbents for heavy metal ions

Huixia Zhu, Shiru Jia*, Tong Wan, Yuanyuan Jia, Hongjiang Yang, Jing Li, Lin Yan, Cheng Zhong

Key Laboratory of Industrial Fermentation Microbiology, Ministry of Education, Tianjin University of Science and Technology, 29 13th Street, TEDA, Tianjin 300457, PR China

ARTICLE INFO

Article history:
Received 27 April 2011
Received in revised form 10 June 2011
Accepted 21 June 2011
Available online 29 June 2011

Keywords:
Biosynthesis
Fe_3O_4
Bacterial cellulose
Nanocomposites
Heavy metal ions

ABSTRACT

In this paper, spherical Fe_3O_4/bacterial cellulose (BC) nanocomposites as adsorbents for heavy metal ions were biosynthesized from *Gluconacetobacter xylinum* by agitation fermentation. A pH controlling embedding method as a new approach was applied to biosynthesize spherical Fe_3O_4/BC nanocomposites. Scanning electron microscopy (SEM) images indicated that the Fe_3O_4 nanoparticles were enwrapped homogeneously in the spherical BC. The spherical Fe_3O_4/BC nanocomposites with 33 wt% ferrous loading had 41 emu/g of the saturated magnetization (σ_s) and 27 Oe of the related coercivity. The adsorption and elution capacities of the spheres for Pb^{2+}, Mn^{2+}, and Cr^{3+} were evaluated. The results indicated that the spherical Fe_3O_4/BC nanocomposites had high adsorption capacities and were recyclable after the elution of heavy metal ions. Compared with conventional preparation procedure for cellulose spheres, spherical Fe_3O_4/BC nanocomposites can be readily prepared without sophisticated steps and have high adsorption and elution capacities.

1. Introduction

In recent years, the industrial and domestic wastewater containing heavy metal ions is responsible for causing several damages to the environment and adversely affecting the health of the people (Matsuto, Jung, & Tanaka, 2004). Natural cellulose derived from plants can be used to prepare cellulose spheres as adsorbent materials for heavy metal ion reclamation (Kumar, Kang, & Hohl, 2001; Liang & Chen, 2007; Liu, Huang, & Deng, 2007; Nagaoka et al., 2002; Rama, Senapati, & Das, 2005). However, the preparation procedure for cellulose spheres involves several sophisticated steps such as basification, aging, carbonization, dissolution, opposing suspension and renewing (Liang & Chen, 2007; Liu et al., 2007), during which environmental pollutants are created such as strong alkali, acid and organic solvents (Nagaoka et al., 2002; Rama et al., 2005).

Bacterial cellulose (BC) consisting of cellulose nanofibrils, is biosynthesized by *Gluconacetobacter xylinum*. The remarkable features of BC, such as high crystallinity and high modulus compared with other sources of cellulose, result in the mechanical improvement of PVA/BC nanocomposites (Millon & Wan, 2006). The high purity and tremendous water holding capability provide good biocompatibility and controllable biosynthesis (Uraki et al., 2007). Chemical sulfation and phosphorylation of BC can be used as potential scaffolds for tissue engineering of cartilage (Svensson et al., 2005). From biosynthesis point of view, there are two fermentation approaches to culture BC. In static fermentation, BC is created in the form of a membrane at the liquid–vapor interface. In agitation fermentation, it can be shaped as spherical bacterial cellulose by controlling the condition of the agitation culture (Czaja, Young, Kawecki, & Brown, 2007; Sani & Dahman, 2010; Yamanaka & Sugiyama, 2000).

Compared with BC membrane, spherical BC with great surface areas and nano-pores has potential applications in bioseparation, heavy metal ion removal from sewage disposal and immobilization reactions. Dead cells and cell debris in BC are also helpful to remove heavy metal ions from sewage disposal, since these substances are rich in chemical functional groups such as carboxyl, phosphoryl, hydroxyl, phosphate and amino groups, which are combinable with heavy metal ions. N, O, P and S as co-ordination atoms are complexed with heavy metal ions and co-ordination complexes were formed (Vieira & Volesky, 2000). To address this need, the Fe_3O_4/bacterial cellulose spheres are used without removing enwrapped dead cells and cell debris.

Since spherical BC with fine nano-pores is easily undermined by traditional recycling process such as filtration or centrifugation, it cannot be properly recollected, which restricts its potential applications. Magnetic separation technology is widely used to separate nucleic acid, protein and other biological macromolecules in biomaterial extraction and purification (Zborowski, Moore, Williams, & Chalmers, 2002). In this technology, the composite containing magnetic particles processes superparamagnetism, so it can be collected under a magnetic field. When the magnetic field is removed,

* Corresponding author. Tel.: +86 022 60601598; fax: +86 022 60272218.
E-mail address: jiashiru@tust.edu.cn (S. Jia).

0144-8617/$ – see front matter © 2011 Elsevier Ltd. All rights reserved.
doi:10.1016/j.carbpol.2011.06.061

the magnetism disappears and the composite can be re-dispersed without damage (Timko et al., 2004).

Superparamagnetic particle materials include Ni, Co, Fe, Fe_2O_3, Fe_3O_4, Fe–Co, and Ni–Fe (Safarik & Safarikova, 2002). Among these, Fe_3O_4 nanoparticles with low mammalian cell toxicity (LD_{50} < 2000 mg/kg) are readily prepared and very stable under culture mediums (Jiles, 2003). Therefore, it is expected that the spherical Fe_3O_4/BC nanocomposites can be designed and biosynthesized.

In this paper, spherical Fe_3O_4/BC nanocomposites were biosynthesized via *G. xylinum* by agitation fermentation. Dead cells and cell debris in the spherical Fe_3O_4/BC nanocomposites were inactivated without removal. The adsorption and elution capacities of the spheres for Pb^{2+}, Mn^{2+}, and Cr^{3+} were evaluated. The results indicated that the spherical Fe_3O_4/BC nanocomposites had high adsorption capacities and can be used repeatedly after the elution of heavy metal ions.

2. Materials and methods

2.1. The fabrication of Fe_3O_4 nanoparticles

Fe_3O_4 nanoparticles were synthesized by co-precipitation from a mixture solution of Fe(II) and Fe(III) salts (Dresco, Zaitsev, Gambino, & Chu, 1999; Ramirez & Landfester, 2003; Zheng, Cheng, Bao, & Wang, 2006). The detailed preparation procedure is as follows: $FeCl_3{\cdot}6H_2O$ (23.5 g) and $FeCl_2{\cdot}4H_2O$ (8.6 g) were weighed and dissolved in deionized water (600 ml) at 30 °C. $NH_3{\cdot}H_2O$ (200 ml of 8 mol/l) was then slowly added into the mixture solution of $FeCl_3$ and $FeCl_2$ with vigorous stirring under N_2 gas to prevent oxidation until the pH reached 10. After precipitation, the Fe_3O_4 nanoparticles were repeatedly washed using deionized water and ultrasonically treated to prevent aggregation until the pH reached 7. Finally, Fe_3O_4 nanoparticles were sterilized at 121 °C for 30 min.

2.2. Biosynthesis of spherical Fe_3O_4/BC nanocomposites

G. xylinum CGMCC No. 2955 was isolated in the Key Laboratory of Industrial Fermentation Microbiology, Tianjin University of Science and Technology, and stored in China General Microbiological Culture Collection Center. The culture medium for BC agitation fermentation consisted of carbon source 25 g/l (Yingbo Biochemical Reagent Co. Ltd., China), peptone 10 g/l (Sigma, America), yeast extract 7.5 g/l (Sigma, America) and disodium phosphate 10 g/l (Sigma, America) at the initial pH value 6.0. For seed culture, *G. xylinum* was inoculated into culture medium (100 ml) in a 500 ml flask on a rotary shaker (Donglian Co. Ltd., China) with 160 rpm of agitation speed and incubated at 30 °C for 24 h (Jia et al., 2004; Tang, Jia, Jia, & Yang, 2010). After incubation, cellulase (2 ml of 10,000 U/ml, Novozymes, Denmark) was added to the culture for enzymolysis at 30 °C for 2 h. The aim of cellulase hydrolysis was to degrade cellulose in the seed liquid, so as to liberate enwrapped cells; therefore uniform BC spheres were produced in the subsequent fermentation stage. *G. xylinum* cells were centrifugally washed with deionized water for three times to remove residual cellulase and then added in 100 ml culture medium with sterilized Fe_3O_4 nanoparticles. After 48 h of fermentation, Fe_3O_4/BC spheres were collected and washed with flowing water to remove residual medium. Then they were boiled in distilled water for 5 min to inactivate the cells.

2.3. Characterization of the spherical Fe_3O_4/BC nanocomposites

The X-ray diffraction (XRD) with CuK_α radiation (Bruker-AXS/D8 Advance) was used to measure the crystallinity of Fe_3O_4 nanoparticles, spherical BC, and Fe_3O_4/BC spheres. XRD data were collected in the 2θ range from 5° to 80°, with a step of 0.02°. The electron field emission scanning electron microscope (FESEM), LEO/1530VP, was applied to observe morphology of the spherical Fe_3O_4/BC nanocomposites. The samples prepared for the SEM experiments were rapidly frozen in liquid nitrogen, and then transferred to a freeze dryer to allow the frozen water in the samples to sublimate. A thin layer of gold was coated on the surface of all samples. The magnetic intensity of spherical Fe_3O_4/BC nanocomposites was measured using Physics Property Measurement System (PPMS-9) Quantum Design.

2.4. The adsorption and elution of Fe_3O_4/BC on Pb^{2+}, Mn^{2+} and Cr^{3+}

The heavy metal salts ($Pb(NO_3)_2$, $MnCl_2{\cdot}4H_2O$ and $Cr(NO_3)_3{\cdot}9H_2O$) were dissolved in deionized water, respectively. The concentration of each ions (Pb^{2+}, Mn^{2+} and Cr^{3+}) in the mixture solution was 4000 mg/l. 120 g of spherical Fe_3O_4/BC nanocomposites in wet weight was evenly divided and loaded in 24 test tubes. 5 g of wet samples in each test tube contained an average 25 mg of dry Fe_3O_4/BC nanocomposites. 24 test tubes were separated into 8 groups. Each group had three test tubes for parallel tests. Each tube was diluted to 10 ml with various concentrations. The final concentrations of Pb^{2+}, Mn^{2+} and Cr^{3+} were 0, 20, 40, 60, 80, 100, 150, and 200 mg/l, respectively, for 8 groups in 24 test tubes. All test tubes were placed in a water bath at 25 °C for 2 h to test the adsorption of Pb^{2+}, Mn^{2+} and Cr^{3+}. Finally, a magnet was used to collect and remove the spheres out of the tube. 1 ml of the upper clear liquid from each test tube was taken and diluted properly to test the concentrations of Pb^{2+}, Mn^{2+} and Cr^{3+}. 0.1 mol/l of sodium citrate was used to elute Pb^{2+}, Mn^{2+}, and Cr^{3+} from the spheres. The above procedure of adsorption and elution was repeated for three times and denoted as the first, second and third adsorption and elution. An atomic absorption spectrophotometer (AA-6800, Shimadzu, Japan) was used to analyze the element content of Fe, Pb, Mn and Cr. The content of Pb^{2+}, Mn^{2+}, and Cr^{3+} was determined. The absorption capacities of Pb^{2+}, Mn^{2+}, and Cr^{3+} were then calculated as follows:

$$Q = \frac{(N-R)\times 10}{1000\times 0.025} = \frac{N-R}{2.5} \quad (1)$$

In Eq. (1), Q refers to adsorption quantity (mg/g); N is the initial concentration of heavy metal ions (mg/l); R refers to the residual concentration of heavy metal ions (mg/l); 10 is the volume of solution (ml); 0.025 is the weight of dry Fe_3O_4/BC nanocomposites.

$$A\ (\%) = \frac{Q\times 0.025}{N\times 0.01}\times 100 = \frac{2.5Q}{N}\times 100 \quad (2)$$

In Eq. (2), A refers to adsorption capacity (%); 0.01 is the volume of solution (l); other terms are same as Eq. (1).

$$B\ (\%) = \frac{W}{Q}\times 100 \quad (3)$$

In Eq. (3), B refers to elution capacity (%); W refers to the eluent concentration of heavy metal ions (mg/g); other terms are same as Eq. (1).

3. Results and discussion

3.1. Biosynthesis of spherical Fe_3O_4/BC nanocomposites

Spherical Fe_3O_4/BC nanocomposites and BC with 3 mm in average diameter were successfully biosynthesized by *G. xylinum* fermentation under the same agitation procedure. Fig. 1 shows that spherical BC is opaque and spherical Fe_3O_4/BC is black due to well dispersed Fe_3O_4 between BC nanofibrils. Fe_3O_4 nanoparticles dispersing in polymer matrix have been reported including

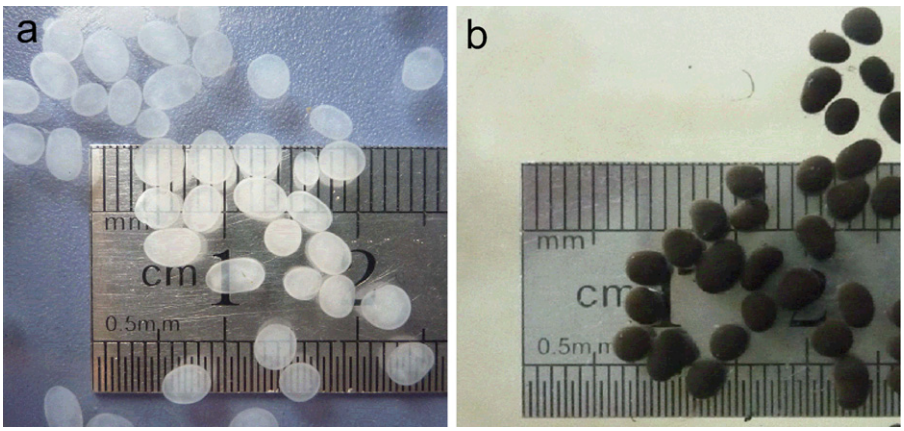

Fig. 1. Photos of spherical BC and spherical Fe_3O_4/BC nanocomposites.

direct compounding, interfacial deposition, and *in situ* polymerization (Deng, Yang, Wang, & Fu, 2003; Ma, Guan, Liu, & Liu, 2005; Sun, Wang, Wang, & Jiang, 2007). However, it is still a challenge to obtain well dispersed Fe_3O_4 nanoparticles during fermentation process. In this study, pH controlling embedding method as a new approach is applied to biosynthesize spherical Fe_3O_4/BC nanocomposites. The proposed scheme of biosynthesis of spherical Fe_3O_4/BC nanocomposites is shown in Fig. 2. During the initial fermentation, the pH of culture medium is adjusted to 6.5, approaching the isoelectric point of Fe_3O_4 nanoparticles, resulting in its aggregation in the initial stage. With fermentation ongoing, the acidity of culture medium continuously increases due to sugar metabolism by *G. xylinum* (Krystynowicz et al., 2002). After 36 h the pH of the culture medium decreases to 4, which is far lower than the isoelectric point, so Fe_3O_4 nanoparticles are dispersed uniformly between BC nanofibrils and no obvious aggregation is observed. The embedded Fe_3O_4 nanoparticles, containing amphoteric hydroxyl groups, form hydrogen bonds with the hydroxyl groups of BC nanofibrils (Jonas & Farah, 1998; Yamanaka & Sugiyama, 2000; Zaar, 1997). During fermentation, the BC nanofibrils are continuously assembled and interlinked to form spheres. Fe_3O_4 nanoparticles are entrained into the spheres under the agitation circumstance.

The relationship between the yield of the spherical Fe_3O_4/BC nanocomposites and the quantity of Fe_3O_4 nanoparticles added into the culture mediums is shown in Fig. 3. Atomic absorption assay is used to measure Fe content. In the initial stage, there is a dramatic increase in the yield of the spherical Fe_3O_4/BC nanocomposites with the addition of Fe_3O_4 nanoparticles. When the dose of Fe_3O_4 nanoparticles is more than 2.5 g/l, the content of Fe in the spherical Fe_3O_4/BC nanocomposites approaches constant and the yield reaches to the maximum level. The content of Fe in the Fe_3O_4/BC nanocomposites is 33 wt%.

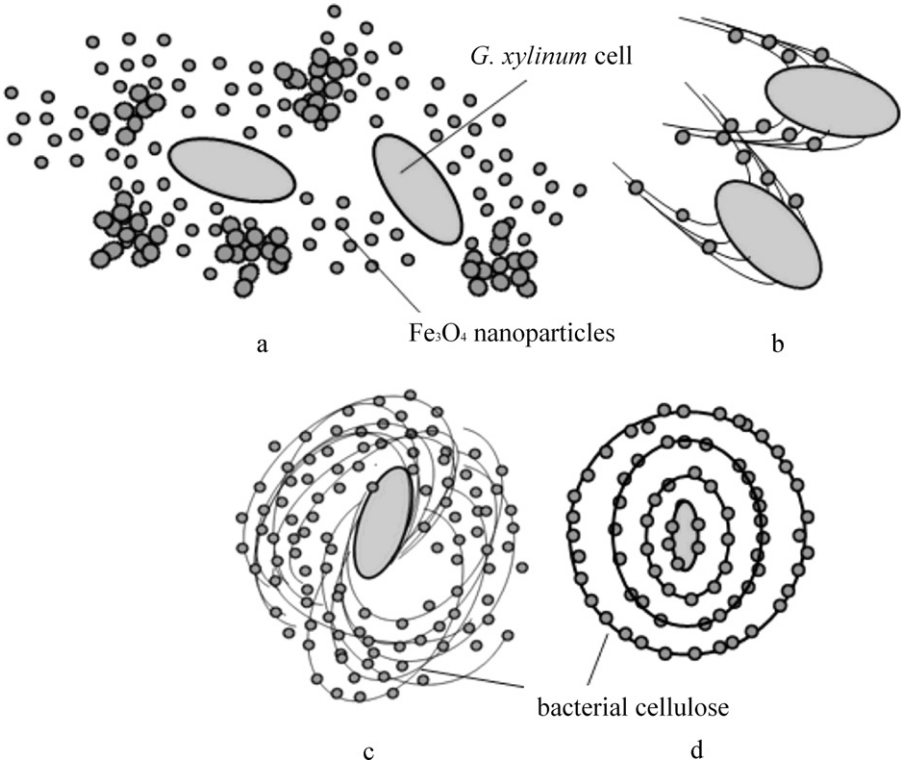

Fig. 2. A schematic diagram of spherical Fe_3O_4/BC nanocomposites. a: Fe_3O_4 nanoparticles dispersing in the medium; b and c: Fe_3O_4 nanoparticles embedded in BC; d. spherical Fe_3O_4/BC nanocomposites.

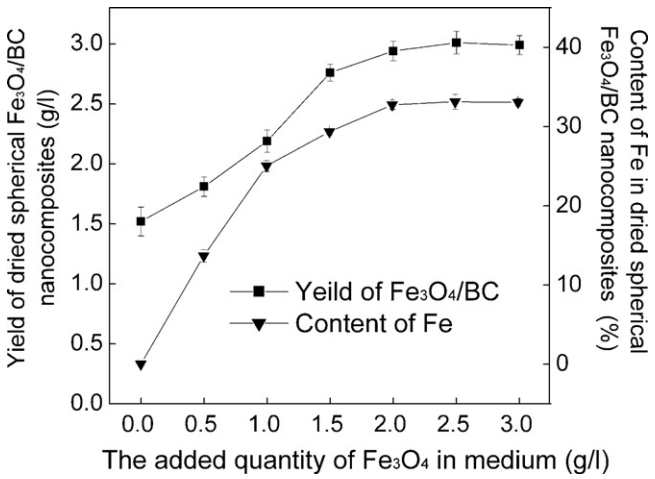

Fig. 3. The yield and content of Fe in spherical Fe_3O_4/BC nanocomposites.

The content of Fe and the size of Fe_3O_4 nanoparticles are related to the saturating magnetic spectroscopy (σ_s) (Buschow, 2008). The magnetic hysteresis loop of the spherical Fe_3O_4/BC nanocomposites is shown in Fig. 4. Increasing the Fe content in Fe_3O_4/BC nanocomposites from 14% to 33%, the corresponding saturated magnetization (σ_s) increases from 12 to 41 emu/g. Under the magnetic field, the spherical Fe_3O_4/BC nanocomposites show good magnetic responsiveness. When the applied magnetic field is removed, their magnetization disappears. Therefore, in this study, 2.5 g/l of Fe_3O_4 nanoparticles corresponding to 41 emu/g of saturated magnetization (σ_s) is fixed for studying adsorption and eluent, at which the spherical Fe_3O_4/BC nanocomposites can devote enough saturated magnetization to magnetic separation (Buschow, 2008).

3.2. X-ray diffraction analysis

The X-ray diffraction patterns of Fe_3O_4 nanoparticles, spherical BC, and spherical Fe_3O_4/BC nanocomposites were obtained by XRD measurements. A comparison of the XRD graphs of samples is shown in Fig. 5. The diffraction peaks of Fe_3O_4 nanoparticle crystalline appear at 18.09°, 29.95°, 35.44°, 43.19°, 57.05°, and 62.61°, which is similar to the peaks of standard Fe_3O_4 nanoparticle crystalline at 18.12°, 30.16°, 35.7°, 43.33°, 57.1°, and 62.98°, corresponding to (2 2 0), (3 1 1), (4 0 0), (4 2 2), (5 1 1), and (4 4 0) of the Fe_3O_4 crystalline face, respectively (Wang, Sun, Sun, & Chen, 2003). According to Scherrer equation $D = k\lambda/(\beta \cos\theta)$, the grain size of Fe_3O_4 nanoparticles is 15 nm, where $k = 0.89$, $\lambda = 0.1542$ nm, $\beta = 0.01418$ of half-peak width at 35.44°.

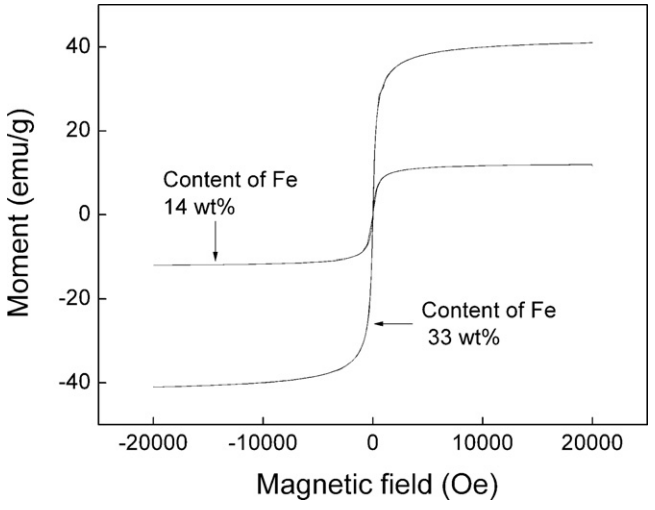

Fig. 4. The hysteresis loops for the spherical Fe_3O_4/BC nanocomposites.

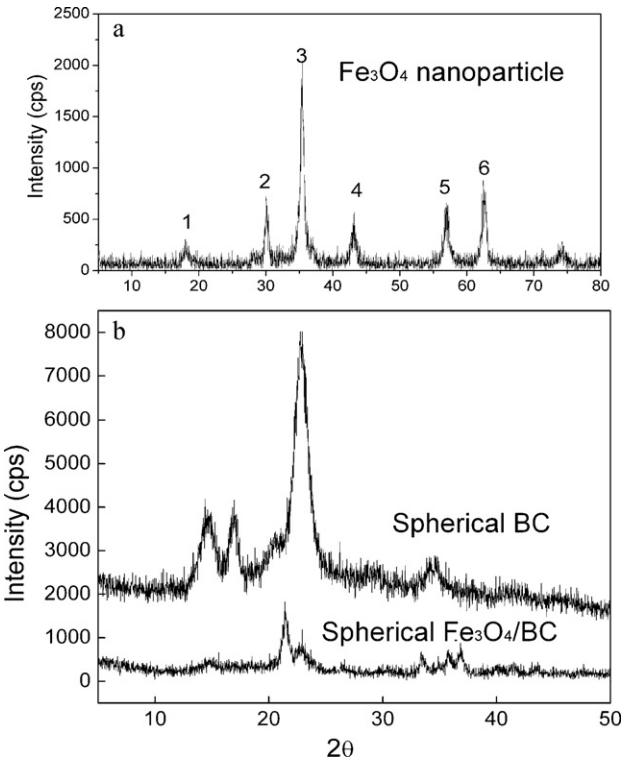

Fig. 5. X-ray diffraction spectra for spherical BC and spherical Fe_3O_4/BC.

The saturating magnetic spectroscopy (σ_s) of the Fe_3O_4 nanoparticles decreases with a reduction in diameter (He et al., 2005; Shen, Fang, Zhou, & Liang, 2004). In this study, the synthesized Fe_3O_4 nanoparticles with 15 nm in size are used for biosynthesis in the culture medium.

The characteristic diffraction peaks of spherical BC appearing at 14.56°, 16.60°, and 22.64° represent a typical (I_α) crystalline of cellulose, which demonstrates that the fabrication of Fe_3O_4 nanoparticles in this study is successful (Fontana et al., 1997; Wang et al., 2003). However, the peaks at 14.56° and 16.60° are not observed in the spherical Fe_3O_4/BC nanocomposites, but a significant peak at 21.45° appeared which might be due to the alteration in size and crystallinity of BC. Moreover, since the diffraction peak intensities of Fe_3O_4/BC nanocomposites are relative low, compared with those of spherical BC, there is an obvious decrease in the crystallinity of the BC in the spherical Fe_3O_4/BC nanocomposites.

3.3. Morphology study of spherical Fe_3O_4/BC nanocomposites

Morphology of Fe_3O_4 nanoparticles enwrapped by the presence of bacterial cellulose is investigated as shown in Fig. 6. As shown in Fig. 6a, bacterial cellulose presents nanofibril network where each fibril is around 50 nm in diameter. Due to the numerous nano-pores in BC, Fe_3O_4 nanoparticles can easily penetrate inside the cellulose network, keeping a close interaction with the nanofibrils. Fe_3O_4 nanoparticles are well known by their granule-like shape, around 15 nm in diameter as shown in Fig. 6b. A large deposition of Fe_3O_4 nanoparticles over the BC surface is noticed. The well dispersed Fe_3O_4 nanoparticles can be seen clearly in Fig. 6b, which is consistent with XRD results. It is believed that some nanoparticles are

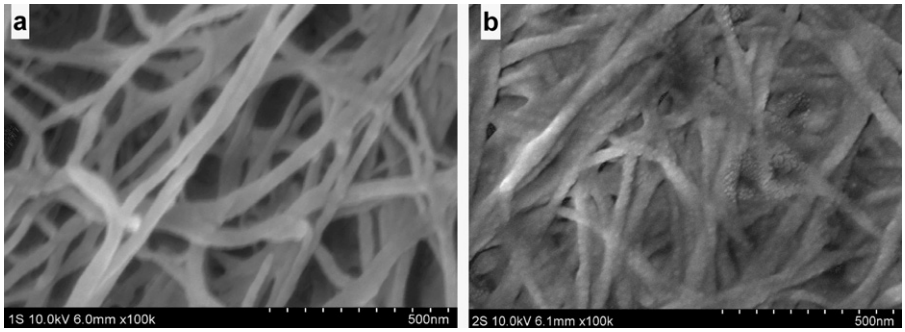

Fig. 6. SEM images of surface morphology of spherical BC on the left (a) and spherical Fe_3O_4/BC nanocomposites on the right (b).

able to penetrate the BC nanofibrils and create a strong interaction with dead cells and cell debris of *G. xylinum*.

3.4. Spherical Fe_3O_4/BC nanocomposites for heavy metal ion removal

Fig. 7 shows the adsorption capacities of the spherical Fe_3O_4/BC nanocomposites for different heavy metal ions (Pb^{2+}, Mn^{2+}, and Cr^{3+}). The adsorption quantities of these heavy metal ions increased with the concentrations of the heavy metal ions. When Pb^{2+} concentration ranges from 0 to 100 mg/ml, the adsorption quantity of Pb^{2+} is proportional to its concentration and the adsorption capacity is higher than 90%. However, the adsorption quantity approaches a constant at 52 mg/g, when Pb^{2+} concentration ranges from 100 to 200 mg/ml and the adsorption capacity is decreased from 90% to 65%.

The Fe_3O_4/BC spheres have a similar behavior for adsorption of Mn^{2+} and Cr^{3+}. The growth of adsorption quantities with ion concentrations shows a trend of initial rapid rising and then mild change. When the concentrations of Mn^{2+} and Cr^{3+} are lower than 60 mg/ml, the adsorption quantities of Mn^{2+} and Cr^{3+} are proportional to their concentrations. In this range, the adsorption capacity of spherical Fe_3O_4/BC nanocomposites is proportional to Mn^{2+} and Cr^{3+} concentrations, and the adsorption capacity of spherical Fe_3O_4/BC nanocomposites increases from 15% to 26% for Mn^{2+} and from 14% to 20% for Cr^{3+}. While the concentration of Mn^{2+} and Cr^{3+} is above 60 mg/ml, the adsorption capacity for Mn^{2+} decreases from 46% to 33% and from 43% to 25% for Cr^{3+}. The adsorption capacity

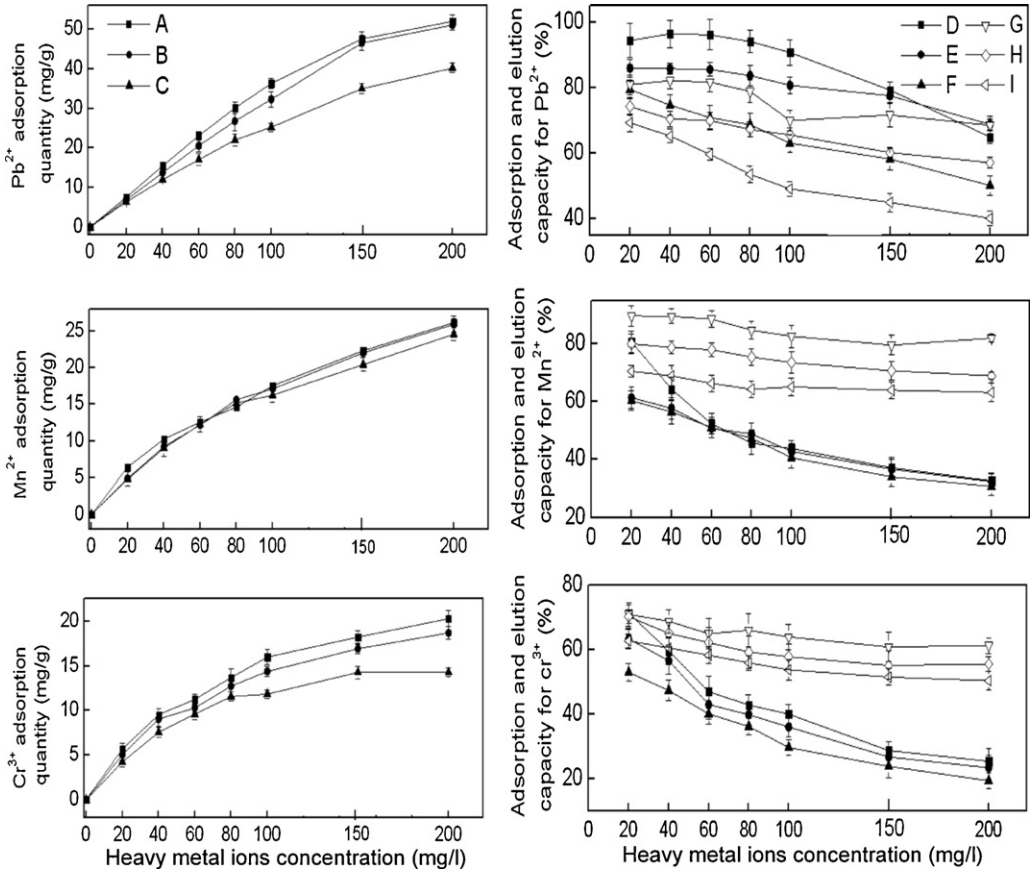

Fig. 7. The adsorption and elution capabilities of the spherical Fe_3O_4/BC nanocomposites for heavy metal ion removal.
A: first adsorption quantity; B: second adsorption quantity; C: third adsorption quantity; D: first adsorption capacity; E: second adsorption capacity; F: third adsorption capacity; G: first elution capacity; H: second elution capacity; I: third elution capacity.

Table 1
Comparison of adsorption quantity of the spherical Fe_3O_4/BC nanocomposites with other materials.

Materials	Study	Adsorption quantity (mg/g)	Reclaim	Eluents
Fe_3O_4/BC spheres	This work	Pb^{2+}, 65 Mn^{2+}, 33 Cr^{3+}, 25	Yes	0.1 mol/l sodium citrate
M. rouxii biomass	Yan and Viraraghavan (2001)	Pb^{2+}, 4 Cd^{2+}, 4 Zn^{2+}, 1	Yes	0.05 mol/l HNO_3
Petiolar felt-sheath palm	Iqbal et al. (2002)	Cd^{2+}, 11 Pb^{2+}, 11 Zn^{2+}, 6	No	
Rice husk ash	Kumar and Bandyopadhyay (2006)	Cd^{2+}, 20 Hg^{2+}, 67	No	
Black gram husk	Saeed and Iqbal (2003)	Cd^{2+}, 50	No	

of these three ions is quite different at the same ion concentration and it is sequenced as $Pb^{2+} > Mn^{2+} > Cr^{3+}$.

Moreover, 0.1 mol/l sodium citrate is used as an eluent to remove the heavy metal ions absorbed by the spherical Fe_3O_4/BC nanocomposites. Fig. 7 shows also the three cycles of adsorption and eluent of Pb^{2+}, Mn^{2+}, and Cr^{3+}. The eluent capacity of the nanocomposites decreases with the adsorption capacity. It is shown that the elution capacity is sequenced as $Mn^{2+} > Pb^{2+} > Cr^{3+}$. The balanced adsorption quantity of spherical Fe_3O_4/BC nanocomposites for Pb^{2+}, Mn^{2+}, and Cr^{3+} increases with their initial concentration, whereas the adsorption capacity for three ions has the opposite trend.

Under stable pH, Fe_3O_4/BC spheres can provide sufficient binding sites to adsorb heavy metal ions in solutions at low ion concentrations. In this range, there is a positive relation between the adsorption capacity and ion concentrations. When the concentration of heavy metal ions is higher than a certain level, all of the binding sites are occupied. Consequently, the adsorption capacity does not increase any more with ion concentrations (Chen, Tendeyong, & Yiacoumi, 1997). After elution, spherical Fe_3O_4/BC nanocomposites are recycled and reused for further adsorption of the same heavy metal ions again. The adsorption and elution capacities of the reused spheres are investigated and the results are shown in Fig. 7. Compared with the results of first test, the adsorption and elution capacities in the second and the third tests for three heavy metal ions slightly decrease. In summary, spherical Fe_3O_4/BC nanocomposites are capable of adsorbing heavy metal ions and are separated and eluted rapidly and easily by sodium citrate. It demonstrates that the absorbent can be recycled and utilized again.

The comparison of adsorption and elution capabilities of spherical Fe_3O_4/BC nanocomposites with other materials provided in references is shown in Table 1 (Iqbal, Saeed, & Akhtar, 2002; Kumar & Bandyopadhyay, 2006; Saeed & Iqbal, 2003; Yan & Viraraghavan, 2001). It demonstrates that adsorption and elution capabilities of spherical Fe_3O_4/BC nanocomposites for the heavy metal ions are much higher than other materials provided in references (Iqbal et al., 2002; Kumar & Bandyopadhyay, 2006; Saeed & Iqbal, 2003; Yan & Viraraghavan, 2001). The high adsorption capabilities may be related to the dead cells and cell debris in the spheres. Dead cells and cell debris in spherical Fe_3O_4/BC nanocomposites are mainly composed of protein, polysaccharide and lipid, which contain a lot of functional groups, such as carboxyl groups, phosphoryl groups, hydroxyl groups, phosphate groups, amino groups, and amide groups. These groups facilitate adsorption by creating covalent bonds with metal ions, resulting in the formation of co-ordination complexes between N, P, O, and S and heavy metal ions (Vieira & Volesky, 2000). These metal ions can also be eluted from the spheres by changing the pH and ionic strength of the chelation (Lazaridis & Charalambous, 2005).

The adsorption and elution capabilities of the spherical Fe_3O_4/BC nanocomposites show that they have promising applications in the industrial sewage treatment. Because it can adsorb heavy metal ions efficiently and be reclaimed by magnetic field, spherical Fe_3O_4/BC nanocomposites can be used not only to cut down the cost of the sewage treatment, but also to avoid secondary pollution to the environment. Although this study describes the spherical Fe_3O_4/BC nanocomposites applied for heavy metal ion adsorption, we also expect that the knowledge gained here could be of considerable interests for bioseparation and enzyme immobilization.

4. Conclusions

In this study, a new Fe_3O_4-nanoparticle-embedding bacterial cellulose sphere (spherical Fe_3O_4/BC nanocomposites) was biosynthesized by *G. xylinum* fermentation. A pH controlling embedding method as a new approach was applied to biosynthesize spherical Fe_3O_4/BC nanocomposites. Dead cells and cell debris were inactivated and reserved in the spherical Fe_3O_4/BC nanocomposites. The XRD and SEM indicated that Fe_3O_4 nanoparticles with 15 nm in the average diameter were distributed uniformly in BC during fermentation. The spherical Fe_3O_4/BC nanocomposites with 33 wt% ferrous loading had 41 emu/g of the saturated magnetization (σ_s) and 27 Oe of the related coercivity. Since the superparamagnetic spherical Fe_3O_4/BC nanocomposites are recycled using magnetic field separation, it can be utilized repeatedly. The adsorption and elution capacities of spherical Fe_3O_4/BC nanocomposites for Pb^{2+}, Mn^{2+}, and Cr^{3+} were evaluated. The results show that the spherical Fe_3O_4/BC nanocomposites can be reused again after the adsorbed heavy metal ions are eluted. The adsorption capacity of these three ions is quite different at the same ion concentrations and it is ranked as $Pb^{2+} > Mn^{2+} > Cr^{3+}$, and the sequence of elution capacity is $Mn^{2+} > Pb^{2+} > Cr^{3+}$.

Acknowledgments

This work was funded by the National Natural Science Foundation of China (No. 20976133), the National Basic Research Program of China (973. Program No. 2007CB 714305), the Foundation for Excellent Doctoral Dissertations of Tianjin University of Science and Technology (No. B201002) and the Foundation of Tianjin Educational Committee (No. 20100602).

References

Buschow, K. H. J. (2008). *Handbook of magnetic materials*. Holland: North Holland Press.

Chen, J. P., Tendeyong, F., & Yiacoumi, S. (1997). Equilibrium and kinetic study of copper ion uptake by calcium alginate. *Environmental Science and Technology*, *31*(5), 1433–1439.

Czaja, W. K., Young, D. J., Kawecki, M., & Brown, R. M. J. (2007). The future prospects of microbial cellulose in biomedical applications. *Biomacromolecules*, *8*(1), 1–12.

Deng, Y. H., Yang, W. L., Wang, C. C., & Fu, S. K. (2003). A novel approach for preparation of thermoresponsive polymer magnetic microspheres with core–shell structure. *Advanced Materials*, *15*(20), 1729–1732.

Dresco, P. A., Zaitsev, V. S., Gambino, R. J., & Chu, B. (1999). Preparation and properties of magnetite and polymer magnetite nanoparticles. *Langmuir*, *15*(6), 1945–1951.

Fontana, J., Joerke, C., Baron, M., Maraschin, M., Ferreira, A., Torriani, I., et al. (1997). *Acetobacter* cellulosic biofilms search for new modulators of cellulogenesis and native membrane treatments. *Applied Biochemistry and Biotechnology*, *63–65*(1), 327–338.

He, Y. P., Wang, Y. P., Li, C. R., Miao, Y. M., Wu, Z. Y., & Zou, B. S. (2005). Synthesis and characterization of functionalized silica-coated Fe_3O_4 superparamagnetic nanocrystals for biological applications. *Journal of Physics D: Applied Physics*, *38*(9), 1342.

Iqbal, M., Saeed, A., & Akhtar, N. (2002). Petiolar felt-seath of palm: A new biosorbent for the removal of heavy metals from contaminated water. *Bioresource Technology*, *81*, 151–153.

Jia, S. R., Ou, H. Y., Chen, G. B., Choi, D., Cho, K., Okabe, M., et al. (2004). Cellulose production from *Gluconobacter oxydans* TQ-B2. *Biotechnology and Bioprocess Engineering*, *9*, 166–170.

Jiles, D. C. (2003). Recent advances and future directions in magnetic materials. *Acta Materialia*, *51*(19), 5907–5939.

Jonas, R., & Farah, L. F. (1998). Production and application of microbial cellulose. *Polymer Degradation and Stability*, *59*(1–3), 101–106.

Krystynowicz, A., Czaja, W., Wiktorowska-Jezierska, A., Gonçalves-Miśkiewicz, M., Turkiewicz, M., & Bielecki, S. (2002). Factors affecting the yield and properties of bacterial cellulose. *Journal of Industrial Microbiology and Biotechnology*, *29*(4), 189–195.

Kumar, U., & Bandyopadhyay, M. (2006). Sorption of cadmium from aqueous solution using retreated rice husk. *Bioresource Technology*, *97*, 104–109.

Kumar, V., Kang, J. C., & Hohl, R. (2001). Improved dissolution and cytotoxicity of camptothecin incorporated into oxidized-cellulose microspheres prepared by spray drying. *Pharmaceutical Development and Technology*, *6*(3), 459–467.

Lazaridis, N. K., & Charalambous, C. (2005). Sorptive removal of trivalent and hexavalent chromium from binary aqueous solutions by composite alginate–goethite beads. *Water Research*, *39*(18), 4385–4396.

Liang, H. X., & Chen, Z. L. (2007). Preparation and property of porous spherical cellulose sorbent. *Chemical Research and Application*, *19*(8), 933–938.

Liu, M. H., Huang, J. H., & Deng, Y. (2007). Adsorption behaviors of L-arginine from aqueous solutions on a spherical cellulose adsorbent containing the sulfonic group. *Bioresource Technology*, *98*(5), 1144–1148.

Ma, Z. Y., Guan, Y. P., Liu, X. Q., & Liu, H. Z. (2005). Preparation and characterization of micron-sized non-porous magnetic polymer microspheres with immobilized metal affinity ligands by modified suspension polymerization. *Journal of Applied Polymer Science*, *96*(6), 2174–2180.

Matsuto, T., Jung, C. H., & Tanaka, N. (2004). Material and heavy metal balance in a recycling facility for home electrical appliances. *Waste Management*, *24*(5), 425–436.

Millon, L. E., & Wan, W. K. (2006). The polyvinyl alcohol–bacterial cellulose system as a new nanocomposite for biomedical applications. *Journal of Biomedical Materials Research Part B: Applied Biomaterials*, *79B*(2), 245–253.

Nagaoka, S., Hamasaki, Y., Ishihara, S.-i., Nagata, M., Iio, K., Nagasawa, C., et al. (2002). Preparation of carbon/TiO_2 microsphere composites from cellulose/TiO_2 microsphere composites and their evaluation. *Journal of Molecular Catalysis A: Chemical*, *177*(2), 255–263.

Rama, K., Senapati, P., & Das, N. (2005). Formulation and *in vitro* evaluation of ethyl cellulose microspheres containing zidovudine. *Journal of Microencapsulation*, *22*(8), 863–876.

Ramirez, L. P., & Landfester, K. (2003). Magnetic polystyrene nanoparticles with a high magnetite content obtained by miniemulsion processes. *Macromolecular Chemistry and Physics*, *204*(1), 22–31.

Saeed, A., & Iqbal, M. (2003). Bioremoval of cadmium from aqueous solution by black gram husk (*Cicer arientinum*). *Water Research*, *37*(14), 3472–3480.

Safarik, I., & Safarikova, M. (2002). Magnetic nanoparticles and biosciences. *Monatshefte Chemical Monthly*, *133*(6), 737–759.

Sani, A., & Dahman, Y. (2010). Improvements in the production of bacterial synthesized biocellulose nanofibrils using different culture methods. *Journal of Chemical Technology & Biotechnology*, *85*(2), 151–164.

Shen, X. C., Fang, X. Z., Zhou, Y. H., & Liang, H. (2004). Synthesis and characterization of 3-aminopropyltriethoxysilane-modified superparamagnetic magnetite nanoparticles. *Chemistry Letters*, *33*(11), 1468.

Sun, Y., Wang, B., Wang, H. P., & Jiang, J. M. (2007). Controllable preparation of magnetic polymer microspheres with different morphologies by miniemulsion polymerization. *Journal of Colloid and Interface Science*, *308*(2), 332–336.

Svensson, A., Nicklasson, E., Harrah, T., Panilaitis, B., Kaplan, D. L., Brittberg, M., et al. (2005). Bacterial cellulose as a potential scaffold for tissue engineering of cartilage. *Biomaterials*, *26*(4), 419–431.

Tang, W. H., Jia, S. R., Jia, Y. Y., & Yang, H. J. (2010). The influence of fermentation conditions and post-treatment methods on porosity of bacterial cellulose membrane. *World Journal of Microbiology and Biotechnology*, *26*(1), 125–131.

Timko, M., Koneracka, M., Kopcansky, P., Ramchand, C. N., Vekas, L., & Bica, D. (2004). Application of magnetizable complex systems in biomedicine. *Czechoslovak Journal of Physics*, *37*(19), 599–606.

Uraki, Y., Nemoto, J., Otsuka, H., Tamai, Y., Sugiyama, J., Kishimoto, T., et al. (2007). Honeycomb-like architecture produced by living bacteria – *Gluconacetobacter xylinus*. *Carbohydrate Polymers*, *69*(1), 1–6.

Vieira, R. H. S. F., & Volesky, B. (2000). Biosorption: A solution to pollution? *International Microbiology*, *3*(1), 17–24.

Wang, J., Sun, J. J., Sun, Q., & Chen, Q. W. (2003). One-step hydrothermal process to prepare highly crystalline Fe_3O_4 nanoparticles with improved magnetic properties. *Materials Research Bulletin*, *38*(7), 1113–1118.

Yamanaka, S., & Sugiyama, J. (2000). Structural modification of bacterial cellulose. *Cellulose*, *7*(3), 213–225.

Yan, G., & Viraraghavan, T. (2001). Heavy metal removal in a biosorption column by immobilized *M. rouxii* biomass. *Bioresource Technology*, *78*(3), 243–249.

Zaar, K. (1997). The biogenesis of cellulose by *Acetobacter xylinum*. *Cytobiologie*, *16*, 1–15.

Zborowski, M., Moore, L. R., Williams, P. S., & Chalmers, J. J. (2002). Separations based on magnetophoretic mobility. *Separation Science and Technology*, *37*(16), 3611–3633.

Zheng, Y. H., Cheng, Y., Bao, F., & Wang, Y. S. (2006). Synthesis and magnetic properties of Fe_3O_4 nanoparticles. *Materials Research Bulletin*, *41*(3), 525–529.